INSTITUTE OF PHYSICS PUBLISHING JOURNAL OF PHYSICS A: MATHEMATICAL AND GENERAL

J. Phys. A: Math. Gen. **36** (2003) 6069–6076 PII: S0305-4470(03)54986-1

Plasma phase transition in dense hydrogen and electron–hole plasmas

V S Filinov[1], M Bonitz[2], P Levashov[1], V E Fortov[1], W Ebeling[3], M Schlanges[4] and S W Koch[5]

[1] Institute for High Energy Density, Russian Academy of Sciences, Izhorskay 13/19, Moscow 127412, Russia
[2] Fachbereich Physik, Universität Rostock, D-18051 Rostock, Germany
[3] Institut für Physik, Humboldt-Universität Berlin, Invalidenstrasse 110, D-10115 Berlin, Germany
[4] Fachbereich Physik, Universität Greifswald, D-17489 Greifswald, Germany
[5] Fachbereich Physik, Philipps-Universität Marburg, D-35032 Marburg, Germany

E-mail: filinov@ok.ru

Received 18 October 2002, in final form 6 December 2002
Published 22 May 2003
Online at stacks.iop.org/JPhysA/36/6069

Abstract

Plasma phase transitions in dense hydrogen and electron–hole plasmas are investigated by direct path integral Monte Carlo methods. The phase boundary of the electron–hole liquid in germanium is calculated and is found to agree reasonably well with the known experimental results. Analogous behaviour is found for high-density hydrogen. For a temperature of $T = 10\,000$ K it is shown that the internal energy is lowered due to droplet formation for densities between 10^{23} cm^{-3} and 10^{24} cm^{-3}.

PACS numbers: 52.25.Kn, 52.65.Pp

1. Introduction

The thermodynamics of strongly correlated Fermi systems at high pressure are of growing importance in many fields, including shock and laser plasmas, astrophysics, solids and nuclear matter, see [1–6] for an overview. Further, among the phenomena of current interest are the high-pressure compressibility of deuterium [7], metallization of hydrogen [8], plasma phase transition etc, which occur in situations where *interaction and quantum effects* and *partial ionization and dissociation* are relevant. Among the early theoretical papers on dense hydrogen concerning the plasma phase transition (PPT), see Norman and Starostin [9], Saumon and Chabrier [10] and Schlanges *et al* [11]; for a more recent overview on the literature, see [12, 13]. These papers are based upon the chemical picture of a partially ionized plasma where the conclusion about the PPT is derived from the non-monotonic behaviour of the isotherms of pressure or chemical potential in a certain density interval.

There are, however, serious questions about the validity of chemical models for high-density quantum plasmas close to pressure ionization and dissociation. Therefore, there is great interest in first-principle simulations of these systems which avoid such approximations. There has been significant progress in recent years in the development of quantum Monte Carlo (QMC), e.g., [14–26] and quantum molecular dynamics (QMD), e.g., [27–29]. In fact, there have been predictions of the PPT from QMC [16] and wave packet MD simulations which, however, have been revised recently [17, 28].

In this paper, we present new QMC results which are based on direct fermionic path integral simulations (DPIMC). Our results for low-temperature dense hydrogen show an instability of the homogeneous plasma state and the formation of droplets. This leads to a significant lowering of the energy. Furthermore, we performed simulations for low-temperature electron–hole plasmas in semiconductors where, unlike hydrogen, phase separation and formation of electron–hole droplets has been clearly observed experimentally [30, 31]. Our results for the phase boundary of the electron–hole liquid in germanium are in good agreement with these data. Due to the similarity of the plasma parameters (coupling, degeneracy, etc) to the situation in dense hydrogen, it is expected that this phenomenon has its counterpart in the PPT in hydrogen.

2. Summary of the path integral Monte Carlo simulations

First, we briefly outline the idea of our scheme. All thermodynamic properties of a two-component plasma are defined by the partition function Z which, for the case of N_e electrons and N_p protons, is given by $Z(N_e, N_p, V, \beta) = \frac{Q(N_e,N_p,\beta)}{N_e!N_p!}$, with $Q(N_e, N_p, \beta) = \sum_\sigma \int_V \mathrm{d}q\, \mathrm{d}r \rho(q, r, \sigma; \beta)$, where $\beta = 1/k_B T$. The exact density matrix is, for a quantum system, in general, not known but can be constructed using a path integral representation [14, 32, 33], $\int_V \mathrm{d}R^{(0)} \sum_\sigma \rho(R^{(0)}, \sigma; \beta) = \int_V \mathrm{d}R^{(0)} \cdots \mathrm{d}R^{(n)} \rho^{(1)} \cdot \rho^{(2)} \cdots \rho^{(n)} \sum_\sigma \sum_P (\pm 1)^{\kappa_P} \mathcal{S}(\sigma, \hat{P}\sigma') \hat{P} \rho^{(n+1)}$, where $\rho^{(i)} \equiv \rho(R^{(i-1)}, R^{(i)}; \Delta\beta) \equiv \langle R^{(i-1)} | \mathrm{e}^{-\Delta\beta \hat{H}} | R^{(i)} \rangle$, whereas $\Delta\beta \equiv \beta/(n+1)$ and $\Delta\lambda_a^2 = 2\pi\hbar^2 \Delta\beta / m_a, a = p, e$. $\hat{H}$ is the Hamilton operator, $\hat{H} = \hat{K} + \hat{U}_c$, containing kinetic and potential energy contributions with $\hat{U}_c = \hat{U}_c^p + \hat{U}_c^e + \hat{U}_c^{ep}$ being the sum of the Coulomb potentials between protons (p), electrons (e) and electrons and protons (ep). Further, σ comprises all particle spins, and the particle coordinates are denoted by $R^{(i)} = (q^{(i)}, r^{(i)}) \equiv \left(R_p^{(i)}, R_e^{(i)}\right)$, for $i = 1, \ldots, n+1$, $R^{(0)} \equiv (q, r) \equiv \left(R_p^{(0)}, R_e^{(0)}\right)$, $R^{(n+1)} \equiv R^{(0)}$ and $\sigma' = \sigma$. This means the particles are represented by fermionic loops with the coordinates (beads) $[R] \equiv [R^{(0)}; R^{(1)}; \ldots; R^{(n)}; R^{(n+1)}]$, where q and r denote the electron and proton coordinates, respectively. The general explicit expression for high-temperature density matrix [14, 24, 34]) can be written as $\langle R^{(i-1)} | \mathrm{e}^{-\Delta\beta\hat{H}} | R^{(i)} \rangle = \int \mathrm{d}\tilde{p}^{(i)}\, \mathrm{d}\bar{p}^{(i)} \langle R^{(i-1)} | \mathrm{e}^{-\Delta\beta\hat{U}_c} | \tilde{p}^{(i)} \rangle \langle \tilde{p}^{(i)} | \mathrm{e}^{-\Delta\beta\hat{K}} | \bar{p}^{(i)} \rangle \langle \bar{p}^{(i)} | \mathrm{e}^{-\frac{\Delta\beta^2}{2}[\hat{K}, \hat{U}_c]} \cdots | R^{(i)} \rangle$. The final expression for the product of the high-temperature density matrices $\sum_{s=0}^{N_e} \rho_s$ is given by

$$\sum_{s=0}^{N_e} \rho_s(\beta) = \left(\prod_{l=1}^{n} \mathrm{e}^{-\beta U_l(\Delta\beta)} \prod_{p=1}^{N_e} \phi_{pp}^l \right) \sum_{s=0}^{N_e} C_{N_e}^s \det \left| \psi_{ab}^{n,1} \right|_s$$

where

$$U_l(\Delta\beta) = \left\{ U_l^p(\Delta\beta) + U_l^e(\Delta\beta) + U_l^{ep}(\Delta\beta) \right\} \Big/ (n+1).$$

Here U_l denotes the sum of proton–proton, electron–electron and electron–proton Kelbg potentials taken for particle positions R^l and $\phi_{pp}^l \equiv \exp\left[-\pi \left|\xi_p^{(l)}\right|^2\right]$. So the density matrix does not contain an explicit sum over the permutations and thus no sum of terms with

alternating sign. Instead, the whole exchange problem is contained in a single exchange matrix given by $\left\|\psi_{ab}^{n,1}\right\|_s \equiv \left\|\mathrm{e}^{-\frac{\pi}{\Delta\lambda_e^2}|(r_a-r_b)+y_a^n|^2}\right\|_s$. In our Monte Carlo simulations this determinant is calculated by the direct methods of linear algebra [22–24]. As a result of the spin summation, the matrix carries a subscript s denoting the number of electrons having the same spin projection. As was suggested by Kelbg the effective potential can be obtained by solving a Bloch equation by first-order perturbation theory. This procedure defines an effective off-diagonal quantum pair potential for Coulomb systems, which depends on the inter-particle distances $\mathbf{r}_{ab}, \mathbf{r}'_{ab}$. As a result of a first-order perturbation calculation, we get explicitly $\Phi^{ab}(\mathbf{r}_{ab}, \mathbf{r}'_{ab}, \Delta\beta) \equiv e_a e_b \int_0^1 \frac{\mathrm{d}\alpha}{d_{ab}(\alpha)} \mathrm{erf}\left(\frac{d_{ab}(\alpha)}{2\lambda_{ab}\sqrt{\alpha(1-\alpha)}}\right)$, where $d_{ab}(\alpha) = |\alpha\mathbf{r}_{ab}+(1-\alpha)\mathbf{r}'_{ab}|$, $\mathrm{erf}(x)$ is the error function $\mathrm{erf}(x) = \frac{2}{\sqrt{\pi}} \int_0^x \mathrm{d}\,t\,\mathrm{e}^{-t^2}$, and $\lambda_{ab}^2 = \frac{\hbar^2\Delta\beta}{2\mu_{ab}}$ with $\mu_{ab}^{-1} = m_a^{-1} + m_b^{-1}$. To save computer time we approximated the two-particle interaction potential by its diagonal elements $(\mathbf{r}'_{ab} = \mathbf{r}_{ab})$ $\Phi^{ab}(|\mathbf{r}_{ab}|, \Delta\beta) \equiv \Phi^{ab}(\mathbf{r}_{ab}, \mathbf{r}_{ab}, \Delta\beta) = \frac{e_a e_b}{\lambda_{ab} x_{ab}}\left[1-\mathrm{e}^{-x_{ab}^2}+\sqrt{[}\pi\}x_{ab}\,(1-\mathrm{erf}(x_{ab}))\right]$, where $x_{ab} = |\mathbf{r}_{ab}|/\lambda_{ab}$, and we underline that the Kelbg potential is finite at zero distance. With these approximations, we obtain the expression for the high-temperature density matrix with accuracy of order $O[(\beta/(n+1))^2]$ and so for the total product of high-temperature matrices with accuracy of order $O[(n+1) * (\beta/(n+1))^2]$ [14, 24]. So for large n the error of this density matrix representation goes to zero and it is possible to check the accuracy of our calculations by calculating with different values of n.

To compute thermodynamic functions, the logarithm of the partition function has to be differentiated with respect to thermodynamic variables. In particular, the internal energy E follows from Q by $\beta E = -\beta\partial \ln Q/\partial\beta$ leading to a rather complicated expression which can be found in [24]. The result is well suited for numerical evaluation using standard Monte Carlo techniques, e.g., [14]. Our procedure has been extensively tested. In particular, we found from comparison with the known analytical expressions for pressure and energy of an ideal Fermi gas that the Fermi statistics is very well reproduced with a limited number of particles ($N \lesssim 100$) and beads ($n \lesssim 20$) for degeneracy up to $n\lambda^3 \lesssim 10$ [22]. Furthermore, we have performed simulations for strongly correlated hydrogen in a wide range of densities and temperatures [22–24]. Below, we present new results for lower temperatures which indicate the existence of phase separation. Besides the simulations for hydrogen, we have performed an extensive analysis of electron–hole plasmas. Some of the results are presented in the following section.

3. Numerical results for electron–hole plasmas

Since the PPT in dense hydrogen is still hypothetical and has not been observed experimentally, it is reasonable to look for other systems where similar conditions exist. A suitable example is electron–hole plasmas in low-temperature semiconductors, for which droplet formation was well established and observed experimentally three decades ago [30, 31]. We, therefore, performed DPIMC simulations for electron–hole plasmas. Below a critical temperature the simulations exhibit anomalously large fluctuations and an unstable behaviour of the pressure. The e–h plasma is found to phase separate and form large droplets [35]. The phase boundary of the electron–hole liquid (e–h droplets) in germanium obtained by our DPIMC method is presented in figure 1 together with the experimental data. We observe good agreement at the wings of the curve, in particular at low density. At higher density (metallic branch) there may be different sources of deviation, in particular not only difficulties in the numerical studies of highly degenerated systems but also the complex band structure of germanium which, in the simulations, was approximated by a two-band parabolic mass model.

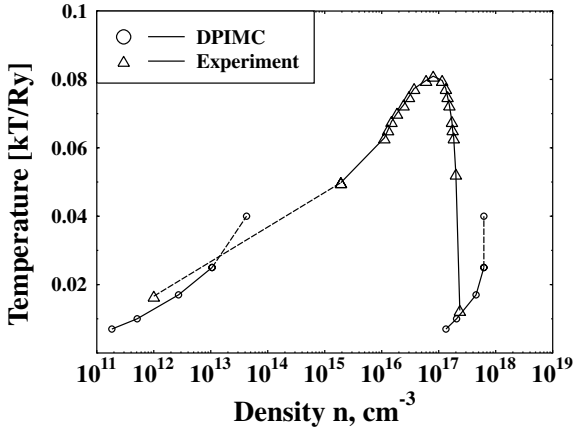

Figure 1. Phase boundary of the electron–hole liquid in bulk germanium [30, 31]. Temperature is presented in units of the exciton binding energy.

4. Numerical results for high-density hydrogen

Let us now come to the numerical results for dense hydrogen. In this paper we concentrate on the internal energy for $T = 10\,000$ K which is well below the critical point of the PPT predicted by chemical models (around $T = 15\,000$ K). Consider first the general behaviour of the energy, figure 2. The overall trend is an increase in the energy with density which is particularly rapid at high densities due to electron degeneracy effects; this is clearly seen from the *ideal plasma* curve (dash-dotted line in figure 2(*b*)). The *nonideal plasma* results show an analogous trend. However, due to the Coulomb interaction the energy is always below the ideal result. The deviations are particularly strong at intermediate densities, between 10^{22} cm^{-3} and 10^{24} cm^{-3}, where the energy becomes negative. This is due to strong Coulomb correlations leading, in particular, to the formation of bound states. This region where correlations and quantum effects are strong is particularly challenging for theoretical description due to the failure of perturbation methods and strong variation of the fractions of free and bound particles. For this reason, here first-principle simulations such as PIMC are of particular value.

In previous papers we concentrated on hydrogen at higher temperatures where the plasma is weakly degenerate and moderately coupled [22–24], and we have obtained good agreement with independent calculations by the restricted PIMC method (RPIMC) [18, 19] for the high densities of interest here, i.e. $n \sim 2.5 \times 10^{23}$ cm^{-3} and temperatures above $T \sim 50\,000$ K. Turning now to lower temperature we find energies which are systematically lower than the RPIMC results for plasma densities in the range of 2.5×10^{22}–10^{24} cm^{-3} which is shown in figure 2(*b*). Our analysis revealed that in the region where the average distance between plasma particles is of the order of the size of a hydrogen molecule the homogeneous plasma state becomes unstable, and many-particle clusters appear which are energetically favourable. Such clusters and the possibility of an inhomogeneous plasma state are apparently excluded in the RPIMC calculations by the additional assumptions (on the nodes of the density matrix) used to reduce the region of integration and the sum over permutations to even (positive) contributions only [17–19]. To verify that the deviations between DPIMC and RPIMC are indeed due to many-particle clusters, we repeated the computations in a slightly modified way: we artificially reduce the region of integration in the partition function to exclude configurations

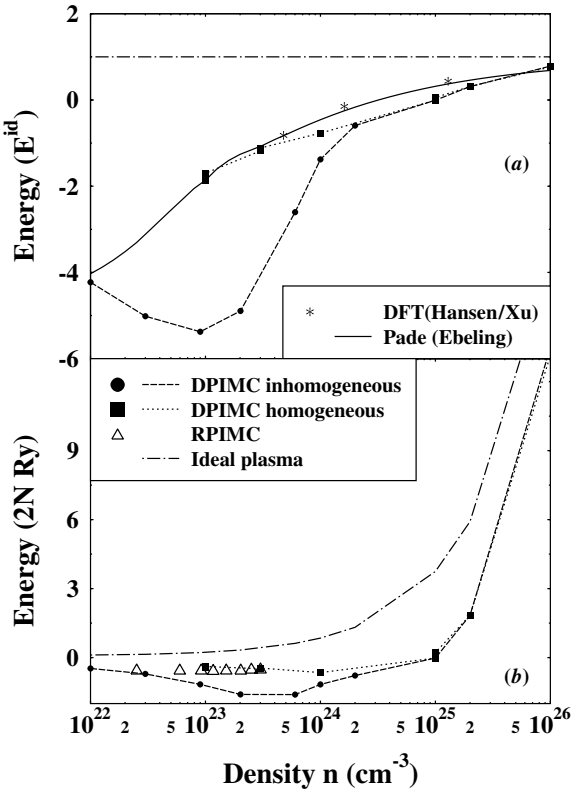

Figure 2. Internal energy of hydrogen for $T = 10\,000$ K, (*a*) normalized to the energy of a noninteracting electron–proton system and (*b*) in units of $2N\cdot$ Rydberg. The curves show results of PACH calculations ('Pade'), our Monte Carlo simulations ('DPIMC'), density functional theory ('DFT') [36] and restricted PIMC data ('RPIMC') of Militzer *et al* [19].

with many-particle clusters, namely configurations, in which distances between three and more particles are smaller than a value $d_{\min}$ varying from 1.3 to $2a_o$. As a result the simulations revealed a plasma consisting of electrons, protons, atoms and molecules which were again homogeneously distributed. At the same time the energy rises significantly and is now very close to the RPIMC result (in the density interval where RPIMC data are available), see curve labelled 'DPIMC homogeneous' in figure 2.

Let us now compare the DPIMC results to data from other approaches. One well-tested method is based on Padé approximations within the chemical picture (PACH), see, e.g., [4, 24] and references therein. These are analytical formulae constructed in such a way that they correctly reproduce the known limiting cases of high and low densities and temperature and interpolate between them. Another independent theoretical method is based on density functional theory (DFT). Recently, Xu and Hansen [36] published data for hydrogen at $T = 10\,000$ K and $r_s \leqslant 1.5$ which are included in figure 2(*a*) together with the Padé results. Evidently, in the high-density limit, PACH and DFT coincide, cf figure 2. This good agreement is not surprising, as the ideal Fermi gas limit is 'built into' each of the approaches. On the other hand, the DPIMC data are systematically below these data for $n > 10^{24}$ cm^{-3} because there electron degeneracy becomes very strong which would require a drastic increase in the number of beads and particles. However, the Padé results (in their present form) do not apply

to situations with low degree of ionization and they exclude larger bound complexes such as molecules and clusters. The DFT data, on the other hand, do not extend to the energy minimum since they also do not include bound states. Interestingly, both Padé and DFT yield strong fluctuations and increasingly unstable results for the thermodynamic functions below densities corresponding to $r_s = 1.5$, which is interpreted by the authors as the precursor of a possible first-order phase transition [36]. In the region of the phase transition not only the equation of state but also other thermodynamic quantities (e.g., the chemical potential isotherms) are expected to have peculiarities such as van der Waals loops [3, 4, 11].

5. Discussion

Let us briefly discuss the implications of our results and note limitations. Our interpretation of the droplets (which are clearly visible in the electron–proton configurations in the simulation box [26, 35]) is that they are a direct indication of a first-order phase transition as discussed in the introduction [9–12]. This is supported by our analogous results for electron–hole plasmas in semiconductors in section 3. Despite this analogy, there are qualitative differences between the two systems. E–h droplets in semiconductor are known to have a stable average size (in the range of micrometres) which is established by the balance of surface energy and recombination where the former tends to increase and the latter tends to reduce the droplet. In dense plasmas, on the other hand, the latter mechanism is missing. This means that coexistence of the two phases—the dense matter in the droplets and the low-density phase between them—may be difficult to observe in a canonical simulation. Therefore, it seems preferable to perform analogous simulations in the grand-canonical ensemble. This is also expected to significantly reduce the instability region and the critical temperature which would then become closer to the experimental result (for the semiconductors) or the theoretical prediction (for hydrogen).

The main point of debate of the present DPIMC results is the low value of the energy in the region of droplet formation, which at minimum is about three times lower than that of molecular hydrogen. This is much lower than one would expect for a macroscopically large system (interestingly, the energy in the semiconductor case is only slightly less than the bi-exciton energy). There are two possible factors which determine the simulation accuracy and which may be responsible: the limited number of particles and the finite number n of beads ($n = 20$ in the simulations). These figures are determined by the presently available computer resources. In particular, the limited number of beads poses problems as the density increases. On the other hand, at densities around $n = 10^{22}$ cm^{-3} where we first observe an instability of the homogeneous state, degeneracy effects are still small and so is the lowering of the energy due to the droplets. We therefore expect that this limitation has no influence on the general existence of the droplets as could be proved by test simulations with $n = 60$. It may certainly affect the observed value of the total energy at higher densities.

The second problem—small size of the simulations (only 56 electrons and protons are presently feasible)—makes it impossible to extrapolate to a macroscopic system. Finite-size effects are, of course, particularly important if the system is inhomogeneous as they overestimate surface energy effects: our simulations yield just a very small number of droplets (typically one to six) each containing 4 to 50 electron–proton pairs most of which are located on the surface of the droplet. This, of course, leads to a lowering of the energy. Therefore, in order to obtain more accurate data for the internal energy of a *macroscopic* two-component plasma at ultrahigh compression, an increase in the simulation size (CPU time) by at least a factor 10 is desirable which should become feasible in the near future.

Acknowledgments

We acknowledge helpful comments on simulation aspects from M E Fisher, H E DeWitt and B Militzer and stimulating discussions with W D Kraeft, D Kremp and R Redmer. This work has been supported by the Deutsche Forschungsgemeinschaft (BO-1366/2) and by a grant for CPU time at the NIC Jülich and the Rostock Linux-Cluster 'Fermion'.

References

[1] Kalman G (ed) 1988 *Strongly Coupled Coulomb Systems* (Oxford: Pergamon)
[2] Kraeft W D and Schlanges M (ed) 1996 *Proc. Int. Conf. on Strongly Coupled Plasmas* (Singapore: World Scientific)
[3] Ebeling W, Kraeft W D and Kremp D 1976 *Theory of Bound States and Ionization Equilibrium in Plasmas and Solids* (Berlin: Akademie)
[4] Kraeft W D, Kremp D, Ebeling W and Röpke G 1986 *Quantum Statistics of Charged Particle Systems* (Berlin: Akademie)
Bonitz M 1998 *Quantum Kinetic Theory* (Leipzig: Teubner)
[5] Filinov A V, Bonitz M and Lozovik Yu E 2001 *Plasma Phys.* **41** 357
Filinov A V, Bonitz M and Lozovik Yu E 2001 *Phys. Rev. Lett.* **86** 3851
[6] Bonitz M (ed) 2000 *Progress in Nonequilibrium Greens Functions* (Singapore: World Scientific)
Bonitz M and Semkat D (eds) 2003 *Progress in Nonequilibrium Greens Functions II* (Singapore: World Scientific)
[7] Da Silva L B *et al* 1997 *Phys. Rev. Lett.* **78** 483
Knudson M D *et al* 2001 *Phys. Rev. Lett.* **87** 225501
[8] Weir S T, Mitchell A C and Nellis W J 1996 *Phys. Rev. Lett.* **76** 1860
[9] Norman G E and Starostin A N 1968 *Teplofiz. Vys. Temp.* **6** 410 (Engl. transl. 1968 *Sov. Phys. High Temp.* **6** 394)
Norman G E and Starostin A N 1970 *Teplofiz. Vys. Temp.* **8** 413 (Engl. transl. 1970 *Sov. Phys. High Temp.* **8** 381)
[10] Saumon D and Chabrier G 1991 *Phys. Rev.* A **44** 5122
[11] Schlanges M, Bonitz M and Tschttschjan A 1995 *Contrib. Plasma Phys.* **35** 109
[12] Beule D *et al* 1999 *Phys. Rev.* B **59** 14177
Beule D 1999 *Contrib. Plasma Phys.* **39** 21
[13] Norman G E 2001 *Contrib. Plasma Phys.* **41** 127
[14] Zamalin V M, Norman G E and Filinov V S 1977 *The Monte Carlo Method in Statistical Thermodynamics* (Moscow: Nauka) (in Russian)
Zelener B V, Norman G E and Filinov V S 1981 *Perturbation Theory and Pseudopotential in Statistical Thermodynamics* (Moscow: Nauka) (in Russian)
[15] De Witt H E 1978 *Strongly Coupled Plasmas* ed G Kalman and P Carini (New York: Plenum)
[16] Magro W R *et al* 1996 *Phys. Rev. Lett.* **76** 1240
[17] Militzer B 2002 Private communication
[18] Militzer B and Pollock E L 2000 *Phys. Rev.* E **61** 3470
[19] Militzer B and Ceperley D M 2000 *Phys. Rev. Lett.* **85** 1890
[20] Filinov V S 2001 *J. Phys. A: Math. Gen.* **34** 1665
[21] Filinov V S, Levashov P R, Fortov V E and Bonitz M 1999 *Progress in Nonequilibrium Greens Functions* ed M Bonitz (Singapore: World Scientific) p 513 (*Preprint* cond-mat/9912055)
[22] Filinov V S, Bonitz M and Fortov V E 2000 *JETP Lett.* **72** 245
[23] Filinov V S, Fortov V E, Bonitz M and Kremp D 2000 *Phys. Lett.* A **274** 228
[24] Filinov V S, Bonitz M, Ebeling W and Fortov V E 2001 *Plasma Phys. Contr. Fusion* **43** 743
[25] Filionv A, Bonitz M and Ebeling W 2003 Accuracy and improvements of the Kelbg potential are analysed *J. Phys. A: Math. Gen.* **36** 5957–62
[26] Filinov V S, Fortov V E, Bonitz M and Levashov P R 2001 *JETP Lett.* **74** 384 (Engl. transl. *2001 Pis. Zh. Eksp. Teor. Fiz.* **74** 422)
[27] Klakow D, Toepffer C and Reinhard P-G 1994 *Phys. Lett.* A **192** 55
Klakow D, Toepffer C and Reinhard P-G 1994 *J. Chem. Phys.* **101** 10766
[28] Knaup M 2002 *PhD Thesis* University Erlangen
[29] Filinov V S, Hoyer W, Bonitz M, Kira M and Koch S W *J. Opt.* B (submitted)
[30] Thomas G A, Rice T M and Hensel J C 1974 *Phys. Rev. Lett.* **33** 219

[31] For reviews, see e.g. Jeffries C D and Keldysh L V (ed) 1988 *Electron–Hole Droplets in Semiconductors* (Moscow: Nauka)
Hensel J C, Phillips T G and Thomas G A 1977 *Solid State Phys.* **32** 88
[32] Filinov V S 1975 *High Temp.* **13** 1065
Filinov V S 1976 *High Temp.* **14** 225
[33] Zelener B V, Norman G E and Filinov V S 1975 *High Temp.* **13** 650
[34] Feynman R P and Hibbs A R 1965 *Quantum Mechanics and Path Integrals* (New York: McGraw-Hill)
[35] Bonitz M 2002 *Physik Journal* **7/8** 69
Bonitz M *et al* 2003 *J. Phys. A: Math. Gen.* **36** 5921–9
[36] Xu H and Hansen J P 1998 *Phys. Rev.* E **57** 211